Published in final edited form as:
Cell Signal. 2008 January ; 20(1): 73–82.

DLG1 is an anchor for the E3 ligase MARCH2 at sites of cell-cell contact

Zhifang Cao[a,b], **Alan Huett**[a,b], **Petric Kuballa**[b], **Cosmas Giallourakis**[a,*], and **Ramnik J. Xavier**[a,b,*]

a*Gastrointestinal Unit, Massachusetts General Hospital, Harvard Medical School, Boston, MA 02114, USA*

b*Center for Computational and Integrative Biology, Massachusetts General Hospital, Harvard Medical School, Boston, MA 02114, USA*

Abstract

PDZ domain containing molecular scaffolds play a central role in organizing synaptic junctions. Observations in Drosophila and mammalian cells have implicated that ubiquitination and endosomal trafficking, of molecular scaffolds are critical to the development and maintenance of cell-cell junctions and cell polarity. To elucidate if there is a connection between these pathways, we applied an integrative genomic strategy, which combined comparative genomics and proteomics with cell biological assays. Given the importance of ubiquitin in regulating endocytic processes, we first identified the subset of E3 ligases with conserved PDZ binding motifs. Among this subset, the MARCH family ubiquitin ligases account for the largest family and MARCH2 has been previously implicated in endosomal trafficking. Next, we tested in an unbiased fashion, if MARCH2 binds PDZ proteins in vivo using a modified tandem affinity purification strategy followed by mass spectrometry. Of note, DLG1 was co-purified from MARCH2, with subsequent confirmation that MARCH2 interacts with full-length DLG1 in a PDZ domain dependent manner. Furthermore, we demonstrated that MARCH2 co-localized with DLG1 at sites of cell-cell contact. In addition, loss of the MARCH2 PDZ binding motif led to loss of MARCH2 localization at cell-cell contact sites and MARCH2 appeared to localize away from cell-cell junctions. In *in vivo* ubiquitination assays we show that MARCH2 promotes DLG1 ubiquitination Overall, these results suggest that PDZ ligands with E3 ligase activity may link PDZ domain containing tumor suppressors to endocytic pathways and cell polarity determination.

Keywords

DLG1; MARCH2; PDZ; Ubiquitination; endosomal trafficking

1. Introduction

The ubiquitin proteosome system is highly conserved and functions as the principal means of targeting cytosolic proteins for degradation. Furthermore, there is emerging evidence that post-translational regulatory modifications can effect cellular localization, protein activity, and

Address correspondence to: Ramnik J. Xavier, Center for Computational and Integrative Biology, Massachusetts General Hospital, Simches Research Building, Rm 7222, Harvard Medical School, Boston, MA 02114. Tel: 617-643-3331, fax: 617-643-3328, E-mail: Xavier@molbio.mgh.harvard.edu.
*Contributed equally as senior authors.

protein-protein interactions. A sequential cascade of reactions catalyzed by an ubiquitin-activating enzyme (E1), several ubiquitin conjugating enzymes (E2) and numerous ubiquitin ligases (E3) transfers the 76 aa ubiquitin moiety to lysine residues resulting in covalent modification of substrates. Whereas mono-ubiquitination appears to modulate protein function as well as regulate protein-protein interactions, poly-ubiquitination generally leads to degradation/targeting to the 25S proteosome. Analogous to kinase reactions, E3 ligases, composed in the majority of circumstances of zinc-binding RING (Really Interesting New Gene) domains, are responsible for substrate specificity. Since E3′s carry the specificity information of the ubiquitination reaction, understanding their behavior is critical for understanding events regulated by ubiquitin *in vivo*. Yet, many aspects of E3 function remain largely unknown, such as the determinants of E3 ligase localization [1,2].

The structural features of PDZ domains permit them to mediate specific protein–protein interactions, in numerous signal transduction pathways including polarity determination, development cues, vesicle transport, ion channel signaling, and synaptic signaling [3–5]. PDZ domains are approximately 90 aa long and recognize c-termini of target proteins in sequence specific manner. In the nervous system, the ubiquitin proteosome system (UPS) appears to intersect with PDZ complexes to regulate diverse synaptic attributes including neurotransmitter release, synaptic vesicle recycling, and the dynamic behavior of the post-synaptic density (PSD), along with the morphological behavior of the dendrites. For instance, a handful of PSD proteins have been found to undergo activity- dependent ubiquitination including several PDZ domain encoding scaffold proteins and/or PDZ protein interacting partners such as SHANK, GKAP, AKAP79, and PSD-95. It has been postulated that UPS-mediated turnover of a few “master organizing” proteins regulates widespread changes at the PSD by modifying distinct subsets of PSD proteins, given that changes in the levels of specific PSD components appear to be co-regulated, accumulating or decline as ensembles with similar kinetics and magnitudes [6–8].

Studies in Drosophila and human models have implicated several inter-related processes including endosomal and vesicular trafficking as critical to the maintenance and development of epithelial cell polarity mediated by evolutionarily-conserved polarity complexes such as *dlg-scribble-lgl* at sites of cellular contacts. A link between the ubiquitin proteosome system, vesicular transport and polarity complexes at sites of cell contacts seems plausible given the role of ubiquitin in endosomal trafficking decisions, but has not been firmly established. Ubiquitination can specify whether proteins enter a recycling pathway in early endosomes or are targeted via the multivesicular body (MVB) for destruction. To date, genetic interactions between these types of tumor suppressors have not been identified, nor has there been direct functional or physical evidence that junctional scaffolds connect to endocytic pathways [9]. Yet, the steady-state levels of architectural transmembrane proteins such as occludins and polarity regulators such as DLG1 are likely to be controlled by recycling versus degradation pathways, using vesicular pathways to maintain appropriate polarization of epithelial cells. For example, a key component of this recycling pathway appears to be the Rab GTPase, Rab13 and possibly its effector JRAB (also known as MICAL-L2). Interestingly, dominant-interfering mutants of Rab13 or JRAB, lead to a loss of functional tight junctions in epithelial cells, suggesting a role in their maintenance [10]. Moreover, Drosophila Crumbs expression is regulated by Rab5-dependent endocytosis; a defect in Rab5 function, which is a component of the early endosomes, leads to abnormal apical expansion in *Drosophila* embryonic epithelial cells where Crumbs is expressed [11].

In this study, we reasoned that a systematic integrative genomic screen for effectors of E3 ligases, which could potentially interact with PDZ proteins, might begin to elucidate the connection between endocytic pathways, vesicular sorting and ubiquitination of the PDZ domain encoding polarity complexes. We identified all genes in the human genome that

encoded both at least one RING domain, and an evolutionarily conserved PDZ binding motif in their carboxy-terminus. Out of 312 genes encoding RING domains, twenty four genes contain conserved PDZ motifs. We have previously shown that almost all known PDZ proteins and bona fide PDZ domain interacting proteins harbor conserved motifs [12]. Using an unbiased proteomics approach to identify binding partners of one such RING domain encoding protein, MARCH2, we characterized a novel interaction with the polarity determining protein DLG1.

2. Materials and methods

2.1. E3 Ligase Encoding Gene Identification and PDZ Binding Motif Conservation

We used the Interpro database which encompasses multiple protein domain/family predictions (ex PFAM, SMART, and Prosite) to identify a unique set of non-redundant set of genes (based on combined computational and manual curation taking into consideration all available information such as protein/DNA pairwise alignments and genomic alignment to the human genome), which encode at least encode at least one RING finger motif C-X_2-C-$X_{9–39}$-C-$X_{1–3}$-H-$X_{2–3}$-C/H-X_2-C-$X_{4–48}$-C-X_2—C: Interpro ID IPR001841. (http://www.ebi.ac.uk/interpro/IEntry?ac=IPR001841). We identified 312 human genes, which encode at least one RING finger motif (see Supplementary Table 1 for complete catalog of genes encoding RING domain(s)). Subsequently, we identified the mouse, dog, rat orthologs using a reciprocal best-hit strategy based ultimately on protein sequence(s) with a BLASTP, BLASTX, TBLASTN with an alignment cutoff of ($E<10^{-10}$). For confirmation, orthologs were also identified in the Inparanoid database (http://inparanoid.sbc.su.se/). The PDZ binding motif (s) criteria are based on three well recognized consensus motifs where the most carboxy terminal amino acid is designated the 0 position: Class I: (X-[S/T]-X-[L/V/I/A]-COOH); Class II: (X-ψ-X- ψ-COOH where ψ indicates hydrophobic residue); and Class III: (X-[D/E]-X-[L/V]-COOH) [3, 5, 12] (see Figure 1). We considered the carboxyl terminus conserved if sequences at positions −2 and 0 of all four species satisfied the consensus motif.

2.2. Microarray Analysis

In order to analyze the expression pattern of genes encoding RING domains in the human, we analyzed a compendium of 79 human tissues/cells profiled by microarray technology. The public version of the GNF human expression atlas version 2 [13] was obtained from Novartis (http://wombat.gnf.org/), including the primary .cel files, which used the U133a Affymetrix chip and a custom chip (GNF1H). The data set contains the expression values of 33,690 probes reflecting normalization of each array to a set of 100 housekeeping genes common to both the U133a and custom GNF1H array. Subsequently, global median scaling across the arrays was performed, yielding expression values across samples for each probe set. The absent/present calls were analyzed, and probe sets with 100% absent calls across all 79 human tissues were not included in the analysis. The data set was further filtered by requiring that a probe set have a threshold value >20 in at least one sample and a maximum–minimum expression value >100. A total of 28,852 reliable probes met the above filtering criteria. For each U133a probe set meeting the above criteria, its corresponding UniGene ID and LocusLink ID were identified based on the combined annotation tables provided at the http://wombat.gnf.org/ and NetAffyx websites (http://www.affymetrix.com). For the custom GNF1H chip, the mRNA/EST used to design the probe set was blasted against the exemplar sequences of the UniGene database (Build 116). Of the 28,852 probe sets, 26,789 mapped to 16,811 UniGene IDs. To represent the human expression profiles of RING genes hierarchical clustering with the centroid linkage method was performed using DCHIP using 1 − r as the distance metric, where r is the Pearson correlation coefficient, with relative expression levels displayed. For the 312 RING domain genes we identified based on their Interpro domain, at least one probe for 218 of the 312 genes was represented on the arrays and met our filtering criteria as well as dCHIP's default filtering

criteria. Heatmaps of hierarchical clustering of tissue expression and correlation values are based on a single probe set per gene chosen at random so as to not bias the visual presentation (Supplemental Figure 2). As shown in Supplemental Figure 2 those RING genes with a conserved PDZ binding motif are identified by a tick mark on the right hand of the heatmap.

2.3. Phylogenetic Analysis of RING Genes Encoding Conserved PDZ domains

To identify gene families among the 24 genes encoding RING domains with conserved PDZ binding motifs, CLUSTALW (http://align.genome.jp/sit-bin/clustalw) was employed using reference protein sequences and default parameters to build a phylogenetic tree derived by neighbor-joining analysis applied to pairwise sequence distances (see Supplemental Figure 1).

2.4. Plasmids and antibodies

Human DLG1 (hDLG1, GenBank accession number: NM_004087) was cloned from lymph node cDNA library into pCMV-3xMyc or pCMV-3xFlag vectors (modified ClonTech pCMV-Myc vector with above epitope and MCS region modifications)). Position 823 in our hDLG1 protein is not residue G (gga) as in NM_004087, but residue E (gaa), which is the same as the human DLG1 genomic sequence and is the corresponding residue in mouse DLG1 and rat DLG1. hDLG1delPDZ1–3 was constructed by deleting aa 224–546.

Flag-tagged human MARCH2 gene was constructed by subcloning the coding sequence of MARCH2 (from Open Biobiosystems) into pCMV5 vector from 5′ BamHI and 3′ SalI. 3xHA-tagged human MARCH2 gene was constructed by subcloning the coding sequence of MARCH2 into pCMV-3xHA vector from 5′ BglII/BamHI and 3′ NotI. MARCH2 tail mutant (mMARCH2) was constructed by replacing the last four residues ETPV with AAAA by PCR. MARCH2A97 was constructed by replacing conserved W97 with A. The double mutant mMARCH2A97 was constructed by replacing conserved W97 with residue A in the mMARCH2 construct. MARCH2SS was constructed by replacing conserved C64, C67, C106 and C109 with S, respectively. Myc-tagged ubiquitin was kindly provided by Dr. M. Scheffner (University of Konstanz, Germany). GFP-tagged rat DLG1 was kindly provided by Dr. C.C. Garner (Stanford University, CA). Sequences of all cloned cDNAs were confirmed by the DNA sequencing by MGH DNA Core.

The antibodies used were: mouse monoclonal anti-hemagglutinin (HA) antibody (Covance, Berkeley, CA); mouse monoclonal anti-Myc antibody (Covance); mouse monoclonal anti-green fluorescent protein (GFP) antibody (Covance); anti-Flag M2 monoclonal antibody (Sigma, Saint Louis, MO)

2.5. Cell culture and transient transfection

Human embryonic kidney 293T (HRK293T) cells, HeLa CCL2 cells and H1299 cells were maintained at 37°C and 5 % CO_2 in Dulbecco's Modified Eagle's Medium (DMEM) supplemented with 10 % fetal calf serum, 100 units/ml penicillin G, and 100 ug/ml streptomycin sulfate. One day before transfection, 1.5×10^6 HEK293ET cells in 2 ml of DMEM medium were plated per well in 6-well plate, or H1299 cells in a 10-cm plate were split 1:3 into 10-cm plates. The cells were transiently transfected with the appropriate amount of plasmids by using Transfectin (Bio-Rad, Hercules, CA) according to the manufacturer's instructions. The amount of transfected plasmids was equalized among different samples by using corresponding empty vector(s). 24 hours later, cells were rinsed in ice-cold PBS and lysed in standard lysis buffer [50 mM Tris-HCl, pH 7.6, 150 mM NaCl, 1 % Triton-X-100, 5 mM EDTA, 10 mM sodium fluoride, 1 mM sodium vanadate, 0.4 mM PMSF, and protease cocktail (1 tablet for 10 ml buffer, Roche)] with rotation for 30 min at 4°C. Insoluble materials were removed by centrifugation at 14,000 rpm for 15 min. The protein concentration of the cleared lysate was determined by the DC protein assay (Bio-Rad).

2.6. Immunoprecipitation and immunoblotting

For immunoprecipitation, cell lysates were incubated with appropriate specific antibodies for 3 hours at 4 °C, and subsequently mixed with antibody affinity gel (goat affinity purified antibody to mouse IgG, ICN Pharmaceuticals, Inc) for an additional 90 min at 4 °C; or cell lysates were incubated with anti-Flag M2-agarose (Sigma, Cat. No. A2220) for 90 min at 4 °C. The immunoprecipitates were washed 3 times with standard lysis buffer. The immunoprecipitated proteins and total cell lysates were resolved by SDS-PAGE, transferred to immobilon-P transfer membranes (Millipore, Bedford, MA) and, immounoblotted with the indicated antibodies. Horseradish peroxidase-conjugated anti-mouse or anti-rabbit antibodies (DakoCytomation California Inc, Carpinteria, CA) were used as secondary reagents. Detection was performed by enhanced chemiluminescence with the Western Lightning Chemiluminescence Regent (PerkinElmer life Sciences, Inc, Boston, MA).

2.7. Generation of stable cell line

T-REx^{TM}-293 tetracycline-inducible cell line (Invitrogen, CA) was used for generating a Flag-CBP-MARCH2A97 stable cell line. Transfection and generation of MARCH2A97 T-REx^{TM}-293 stable cell line were performed according to the pcDNA^{TM}4/TO system user's manual (Invitrogen) with the following modification. The pcDNA^{TM}4/TO vector was modified to contain a Flag cassette followed by a CBP cassette upstream of MARCH2A97. Selection with Zeocin (100 ug/ml) began one day after transfection. Individual clones of Flag-CBP-MARCH2A97 expressing cells were screened for inducible expression by western blot analysis with anti-Flag antibody.

2.8. Tandem affinity purification

Sixty 150-mm plates of T-REx^{TM}-293 tetracycline-inducible cell line only and sixty 150-mm plates of Flag-CBP-MARCH2A97 T-REX^{TM}-293 stable cells were grown to 70% confluency and treated with 80 ng/ml tetracycline (final concentration in culture) for 2 days before harvesting the cells, respectively.

Cellular extracts were prepared by lysing cells in lysis buffer [50 mM Tris-HCl, pH7.6, 150 mM NaCl, 0.5 mM EDTA, 10% glycerol, 0.5% Nonidet P-40, 0.5 mM DTT, 0.4 mM PMSF, 1 mM $NaVO_4$, 10 mM NaF, and protease inhibitor tablets (Roche)] followed by homogenization by 15 strokes in a tight-fitting Dounce homogenizer following by two freeze-thaw cycles. Total lysates were centrifuged at 12,500 rpm in a Beckman JA25.50 rotor for 30 min at 4°C. The cleared lysate was incubated with 250ul anti-Flag M2 affinity beads (Sigma) for 4 hours at 4°C. Beads and bound proteins were transferred to a 1.5 ml tube and washed 3 times with lysis buffer, 3 times with calmodulin binding buffer [50 mM Tris-HCl, pH 7.6, 150 mM NaCl, 0.1% Nonidet P-40, 0.1 mM DTT, 1 mM MgOAc, 1mM Imidazole, 2 mM $CaCl_2$, 0.4 mM PMSF, 1 mM $NaVO_4$, 10 mM NaF, and protease inhibitor tablets (Roche)]. The protein complex was eluted with calmodulin binding buffer containing 0.5 mg/ml Flag peptide (Sigma) by incubating for 15 min at 4°C with end-over-end mixing. The eluate was recovered by centrifugation at 2,000 rpm for 30 seconds. The elution was repeated. The two eluates were pooled and incubated with 50 ul of calmodulin Sepharose 4B beads (Amersham Biosciences) for 1 hour at 4°C. The calmodulin beads were then washed 3 times with calmodulin binding buffer at room temperature and eluted with boiling sample buffer. MARCH2A97 and associated proteins were separated by SDS-PAGE and stained using the Colloidal Coomassie blue stain GelCode Blue (Pierce). The bands were cut out of the gel and sent for MS analysis (Taplin Biological Mass Spectrometry Facility, Harvard Medical School, Boston).

2.9. Microscopy and image analysis

HeLa CCL2 cells were seeded at a density of 1×10^5 cells per well on 18mm glass coverslips in 12-well plates and allowed to grow for 24 hours in DMEM supplemented with 10% fetal calf serum. Transfections were performed with Lipofectamine 2000 according to the manufacturer's instructions. All wells received 1μg of rat DLG1-GFP (rDLG1-GFP) along with sufficient MARCH2-Flag constructs and Flag vector to ensure comparable expression levels of different constructs, either: 2μg empty Flag vector; 1μg MARCH2-Flag wild-type with 1μg empty Flag vector; 2μg mMARCH2-Flag; or 0.5μg MARCH2A97-Flag with 1.5μg empty Flag vector.

After 24 hours, cells were fixed with 4% formaldehyde in PBS for 15 minutes at room temperature, permeablized with 0.1% Triton X-100, 1% BSA in PBS for 5 minutes and washed twice in PBS. Flag-tagged proteins were visualized with mouse anti-Flag M2 (Sigma, MI) followed by Alexa Fluor 568-conjugated goat anti-mouse secondary antibody (Invitrogen, CA), diluted in PBS at 1:500 and 1:200 respectively. Actin was visualized with Alexa Fluor 633-conjugated phalloidin (Invitrogen). Following staining, coverslips were extensively washed, mounted in Aqua Polymount (Polysciences, PA) and imaged using a BioRad Radiance 2000 confocal microscope (Carl Zeiss Inc, NY).

Cell-cell junctions were selected by locating actin-rich cell-cell contacts and a 0.2 μm optical section was taken through the central plane of the junction. Care was taken to maintain constant microscope settings to ensure fluorescence intensities were directly comparable between images. Images were analyzed using LSM Image Browser (Carl Zeiss Inc) and Adobe Photoshop (Adobe Systems Inc, CA).

3. Results

3.1. A Genome-Wide Identification of E3 RING Ligases as Potential PDZ Domain Interactors

A genome-wide comparative genomics analysis of RING E3 ligases was conducted to search for those ligases harboring PDZ binding motifs. We had previously shown that 96% of known/literature documented PDZ ligands have a conserved PDZ binding motif, suggesting that conservation of a PDZ binding motif can act as a reasonable parsing mechanism to distinguish those proteins, which can or cannot bind directly PDZ domains [12]. Towards this goal, we compiled a catalog of 312 human genes, which encode at least one RING finger motif C-X2-C-X9–39-C-X1–3-H-X2–3-C/H-X2-C-X4–48-C-X2—C using the interpro ID IPR001841 (see Figure 1 and Supplemental Table 1 for a complete annotation). Using this RING gene compendium, we next asked for each of these 312 genes, whether they encoded proteins which have a conserved PDZ binding motif in their carboxyl terminus in three additional mammalian species: mouse, rat, and dog. A restricted set of 24 genes was identified encoding RING domains and harboring conserved PDZ binding motifs. The 24 proteins were aligned across their entire length and clustered to analyze whether they fell into gene families or represented very distinct RING domain proteins. Interestingly, six of the 24 genes belong to the transmembrane MARCH family of E3 ligases originally identified as E3 ligases in Kaposi-sarcoma, pox and gamma-2-herpes viruses, and utilized to downregulate MHC-I expression for immune evasion (Supplemental Figure 1) [14]. In addition, we examined the 312 E3-ligase encoding genes across 79 tissue/cell lines to define the expression profiles of these 24 genes relative to other E3 ligases that might provide insight as to their function, revealing modules of co-expressed E3 ligases in various tissues (Supplementary Figure 2). We chose to address whether one of the MARCH family members, MARCH2, interacted with PDZ proteins. Although little is known about the physiological function of MARCH2, we focused on its ability to bind PDZ proteins given a variety of observations including: 1) its broad mRNA expression profile; 2) transmembrane properties, since PDZ ligands are over-represented in

transmembrane proteins; 3) its previously demonstrated binding to syntaxins, which have been implicated in polarity determination in Drosophila and humans and; 4) the reduced abundance of MARCH2 mRNA observed in epithelial cancers such as bladder, prostate, and colorectal cancer (see Supplemental Figure 3) [14–16].

3.2. Proteomics Identification of MARCH2 Protein Complexes include PDZ Domain Protein (s) in Epithelial Cells

In order to test the hypothesis that PDZ proteins might interact with MARCH2 *in vivo* in an unbiased fashion, we designed a strategy which took into account the potential challenges of capturing protein complexes in the context of E3 ligases [17]. In this regard, we attempted to rationally modify MARCH2 such that its E3 ligase activity would be attenuated.

Specifically, we chose to mutate the W97 residue in MARCH2, located in the RING domain, which is conserved among MARCH family proteins and also conserved in their viral homologues. Previously, when this equivalent tyrosine (W) residue was changed to alanine (A) in a viral K3 ubiquitin ligase, the protein could no longer downregulate MHC class I molecules, but still could bind to non-ubiquitinated MHC class I molecules. The corresponding residue replacement in the K5 RING domain can partially rescue MHC class I downregulation [17]. Therefore, we mimicked the K3 mutation and replaced W97 residue with alkaline (A) in MARCH2 (MARCH2A97). We hypothesized that such a modification of MARCH2 would allow retention of MARCH2 associated proteins, but reduce target ubiquitination, thereby increasing the chances of finding binding partners and substrate(s) of MARCH2.

We applied a combination of tandem affinity purification (TAP), with a tetracycline-inducible HEK293 cell system, to express Flag and CBP tagged MARCH2A97 and then captured MARCH2A97 and associated proteins by two rounds of immunoprecipitation. Cell extracts containing the expressed TAP-tagged protein were subjected to two-step purification. First, cell extracts were incubated with Flag beads to capture Flag-tagged protein and interactors. The captured complexes were eluted by incubation with Flag peptide. Second, the Flag eluate was further purified by incubation with calmodulin sepharose 4B beads. After washing, highly purified protein complexes are eluted with SDS-PAGE loading buffer and the captured proteins were identified by MALDI mass analysis (Figure 3 and Supplemental Table 2).

We analyzed four bands by mass analysis (Supplemental Table 2). Band 5 corresponded to the expected molecular weight of Flag-CBP-MARCH2A97 and reacted positively to anti-Flag antibody in a western blot (data not shown). Bands were observed above band 1 in the MARCH2A97 lane. However, there were weak bands of the corresponding molecular weights in the control lane, so these bands were not analyzed. Among the identified proteins, we detected hDLG1, a PDZ domain containing protein, from both band 1 and band 2 (Supplemental Table 2).

3.3. The PDZ Binding Motif of MARCH2 Interacts with the PDZ Domain of DLG1 in HEK293T cells

Given the presence of a conserved Class I PDZ binding motif in MARCH2 and identification the PDZ domain encoding protein hDLG1 as part of a MARCH2 complex, we tested for a direct interaction between hDLG1 and MARCH2. Importantly, we found MARCH2A97 was able to bind to full-length hDLG1 in HEK293T cells by co-immunoprecipitation. Next, we ascertained if the PDZ domains of hDLG1 mediated an interaction with MARCH2. We found that although full-length hDLG1 could be co-immunoprecipitated with MARCH2, a hDLG1 deletion mutant lacking the three PDZ domains, hDLG1delPDZ1–3, did not interact (Figure 4A). In addition, we established that the Class I PDZ binding motif of MARCH2AW97 was required for interaction with hDLG1 based on co-immmunoprecipitation (Figure 4B). Taken

together, these results corroborate the finding that endogenous hDLG1 can associate with MARCH2 in HEK293T, as identified by proteomics methods, and furthermore, establish this interaction is likely the result of the PDZ domains of hDLG1 interacting with the carboxy terminal PDZ binding motif of MARCH2.

3.4. DLG1 and MARCH2 Co-localize in Epithelial Cells to Sites of Cell-Contact

Since a GFP-tagged human version of hDLG1 expressed at an extremely low level in HeLa cells, we used a GFP-tagged rat DLG1 (rDLG1) to perform immunostaining analysis since this construct gives robust signal for immunofluorescence experiments as previously reported [18,19]. HeLa cells co-transfected with empty Flag vector and rDLG1-GFP showed bright green fluorescence, with a concentration of rDLG1-GFP signal at sites of cell-cell contacts, consistent with previously published results [20,21] (Figure 5A). Cells expressing Flag vector alone, exhibited consistently low levels of diffuse Flag cytoplasmic staining. This background was used to set the lower detection limits for laser scanning confocal microscopy. Subsequently, cells co-transfected with rDLG1-GFP along with wild-type Flag-MARCH2 exhibited several phenotypes including: 1) a markedly overall lower level of GFP fluorescence; 2) a loss of rDLG1-GFP from cell-cell contacts and; 3) often showed redistribution of rDLG1-GFP to concentrated signal foci in a perinuclear distribution (Figure 5B, arrowed). When co-transfected with wild type rDLG1-GFP, Flag-MARCH2 appeared to be cytoplasmic in most cells and colocalization at cell-cell contact sites were observed. Frequently small, but brightly-stained foci of MARCH2 were observed to colocalize with GFP-bright rDLG1 perinuclear foci. (Figure 5A middle panel, arrowed).

3.5. Mutation of the PDZ Binding Motif of MARCH2 Abrogates DLG1 Co-localization and Leads to Polarization of MARCH2 Localization

In contrast to wild-type MARCH2-Flag, a mMARCH2-Flag (lacking a PDZ consensus binding motif) did not cause a significant reduction in rDLG1-GFP signal and cells maintained cell-cell contact concentrations of GFP-rDLG1 similar to those observed in vector controls (Figure 5A bottom panel). Strikingly, mMARCH2-Flag appeared to localize to opposite poles with respect to sites of cell-cell contacts and hence away from the greatest concentrations of rDLG1 (Figure 5A bottom panel). In addition, co-expression of mMARCH2-Flag did not cause rDLG1-GFP to be redistributed to perinuclear foci. To further investigate the relationships between MARCH2-DLG1 binding, degradation, and cellular location we utilized two ligase activity dominant-negative forms of MARCH2, MARCH2SS and MARCH2A97. Cells co-transfected with rDLG1-GFP and MARCH2A97-Flag or MARCH2SS-Flag retained high levels of rDLG1-GFP fluorescence and cell-cell contact enrichment, despite comparable levels of MARCH2SS, MARCH2A97 and wild type MARCH2 expression (Figure 5B top vs middle + bottom panels). Importantly, in contradistinction to both wild-type MARCH2-Flag and the PDZ-tail mutant mMARCH2-Flag, ubqituitin E3 ligase-impaired MARCH2A97-Flag and MARCH2SS-Flag co-localized with rDLG1-GFP at sites of cell-cell contact. Furthermore, no perinuclear rDLG1-GFP was observed in cells co-expressing MARCH2SS-Flag or MARCH2A97-Flag. These results suggest that DLG1 is required to anchor MARCH2 at sites of cells contacts, but the duration of MARCH2 at sites of contacts is modulated by the MARCH2 E3 ligase activity

3.6. The PDZ Binding Motif of MARCH2 is required for efficient Ubiquitination of DLG1 by MARCH2 *in vivo*

Previously, it had been shown that MARCH2 can function as an E3 ligase *in vitro* [14]. We therefore explored whether DLG1 can be ubiquitinated by MARCH2. Although in the past, it has been suggested that E6AP ubiquitin ligase can function as a E3 ligase for DLG1, the functional consequence of DLG1 ubiquitination, as well as the ability of other E3 ligases to

modulate the stability of DLG1 under various contexts, remain unclear [22,23]. In order to assess if MARCH2 can catalyze ubiquitination of hDLG1 we employed H1299 cells to perform *in vivo* ubiquitination assay. As shown in Figure 6, while ubiquitination of hDLG1 occurred with co-expression of wild type MARCH2, a version of MARCH2, mMARCH2, which cannot interact with hDLG1, does not appear to promote the ubiquitination of hDLG1. This indicated that interaction of MARCH2 with hDLG1 is required for efficient ubiquitination of hDLG1 under these experimental conditions. We next examined the requirement for the catalytic activity of MARCH2 to mediate hDLG1 ubiquitination. In this regard, RING domain dominant negative mutants of MARCH2 including MARCH2SS and MARCH2A97, significantly reduced MARCH2 mediated ubiquitination of hDLG1.

4. Discussion

In this manuscript we have integrated computational strategies with proteomics to begin to elucidate the interaction between PDZ domain encoding proteins and the family of proteins encoding RING domain E3 ligases. Systematic analysis of expression patterns of a genome-wide collection of E3 ligases at high resolution across 79 cell and tissue types revealed a subset of E3 ligases(n=24) as targets for further characterization as PDZ ligands. Proteomic analysis revealed a novel interaction between PDZ ligand MARCH2 and PDZ domain protein DLG1.

We focused on the RING motif since this is the predominant domain which can act as an E3 ligase, although a more limited number of proteins containing the alternative E3 ligase domains including HECT (homologous to E6-associated protein C-terminus n=29) or a U-box (IPR003613; n=15) which is a modified RING domain containing domain [24].

As a result of integrating RING domain motifs with conservation of PDZ binding motif on a genome-wide basis, we were able to computationally predict that 24 of the 312 E3 ligases are high probability interactors with PDZ domains. Strikingly, the MARCH family of transmembrane E3 ligases contributed to the largest fraction of E3 ligases which met our computational filtering criteria (25% or 6/24), suggesting that as a whole these E3 ligases might be important regulators of PDZ proteins or vice versa (ie. that PDZ domains play a significant role in regulating the activity and/or localization of these E3 ligases). This is reminiscent of the functional interaction of PDZ proteins with transmembrane proteins with other classes of genes with catalytic activity as reflected in the recent identification of a family of transmembrane palmitoytansferases which modulate PDZ proteins [25,26].

In addition, to providing a genome wide annotated resource of E3 ligases, we have also developed new protocols and reagents for efficient purification of protein complexes in general that can be applied to elucidate PDZ complexes in vivo. Compared to the classical TAP approach, our strategy simplifies the purification process by eliminating the TEV cleavage step. In addition, the use of the smaller Flag-tag instead of protein A may present less expression burden and potentially a lower level of steric interference with endogenous interactions. We confirmed our computational and experimental approach to elucidate PDZ interaction networks, by providing evidence that E3 ligase MARCH2 interacts with DLG1 and promotes the ubiquitination of DLG1.

Prior to this study, there have only been limited studies examining the connection of E3 ligases harboring carboxy terminal PDZ binding motifs and proteins encoding PDZ domains in normal physiology. Specifically, it had been shown in neurons that PARKIN (OMIM: 602544), responsible for autosomal recessive juvenile parkinsonism, interacts via its PDZ binding motif with CASK. In this report experimental data support a model whereby CASK could modulate PARKIN cellular localization, but was not directly ubiquitnated by PARKIN [27]. In contrast, PDZ proteins such as DLG1 and Scribble interact with the PDZ binding motif of the E6 protein

from high-risk human papillomavirus (HPV, responsible for human cervical cancer), which acts as an E3 ligase, leading to destruction of these PDZ proteins and disorganization of epithelial structures [23]. These studies further demonstrate that E3 PDZ ligands to PDZ domain interactions may have distinct consequences, ranging from destruction of the PDZ domain encoding protein, to alter trafficking of the E3 ligases, which cannot be predicted necessarily *a prior*.

Consistent with previous studies, DLG1 is distributed throughout the cytoplasm and cell-cell adhesion sites in epithelial cells. Increased expression of MARCH2 repositions the cellular distribution of DLG1 and consistently reduced the expression of DLG1 at sites of cell-cell contact. MARCH2 localization is consistent with a previous report that demonstrated MARCH2 is enriched at the membrane by biochemical fractionation studies in Hela cells, and at the leading edges microscopically in CHO cells [16]. The MARCH2 mutant that lacks the PDZ tail relocalizes away from cell-cell contact sites. Importantly, co-expression of the MARCH2 ring finger mutants did not alter the DLG1 localization at sites of cell – cell contact.

At a biochemical level, the function of MARCH2 was assessed by the ability of catalytic and PDZ binding mutants, in comparison to wild type MARCH2, to promote ubiquitination of DLG1 when expressed transiently in H1299 cells. In the absence of the PDZ ligand motif MARCH2 fails to interact and promote ubiquitination of DLG1. Further, we show that MARCH2 ring finger domain mutants significantly reduce the ubiquitination of DLG1 in epithelial cells. The residual ubiquitination of DLG1 observed in the catalytic mutant only experiments, may reflect the possibility that the catalytic mutant MARCH2 might heterodimerize with endogenous MARCH2. This possibility can only be eliminated by eventual testing in MARCH2 knockout cells. Indeed, MARCH-IX has been shown to form homodimers [28]. In addition, some E3 ligases beyond MARCH-IX can form heterodimers. For example, Mdm2 is an E3 ligase for p53, but the E3 ligase MdmX does not appear as an E3 ligase for p53. Yet, MdmX can form a heterodimer with Mdm2. This Mdm2/MdmX dimer can rescue the E3 ligase activity of E3 ligase activity defective mutants of Mdm2 [29]. Together these observations suggest that the MARCH2 PDZ binding motif is required to anchor it to sites of cell-cell contacts, where then its catalytic activity maybe targeted to PDZ proteins such as DLG1 or other polarity proteins..

To date, the MARCH family of proteins has largely been studied in the context of the modulating the levels of MHC I and II molecules [14,30,31]. In addition, MARCH2 binds syntaxin 6, where in Drosophila a syntaxin mutant *avalanche* which is a tumor suppressor has been strongly implicated in epithelial polarity via endocytic processes [11]. Taken together, these findings suggest that MARCH2 may function as a molecular bridge with ubiquitin ligase activity connecting endocytic tumor suppressor proteins such as syntaxins to PDZ domains polarity determining scaffold protein DLG1. Future experiments are aimed at understanding how MARCH2 might control epithelial polarity through regulation of endocytosis and recycling of polarity determinants, and the consequence of loss or gain of MARCH2 expression in epithelial tumors (Supplemental Figure 1), may yield significant insights into mechanisms of normal epithelial morphogenesis and tumorigenesis.

Supplementary Material

Refer to Web version on PubMed Central for supplementary material.

Acknowledgements

We thank Ian Rosenberg and Aimee Landry for critical review of this manuscript. We thank the Brain Seed lab and Michael Fitzgerald lab members for helpful comments. This work was supported by grants from MGH development fund, CSIBD pilot feasibility grant (DK43351) to R.J.X and a Crohn's and Colitis Felllowship to C.G.

References

1. Kerscher O, Felberbaum R, Hochstrasser M. Annu Rev Cell Dev Biol 2006;22:159–180. [PubMed: 16753028]
2. Mukhopadhyay D, Riezman H. Science 2007;315(5809):201–205. [PubMed: 17218518]
3. Sheng M, Sala C. Annu Rev Neurosci 2001;24:1–29. [PubMed: 11283303]
4. Macara IG. Nat Rev Mol Cell Biol 2004;5(3):220–231. [PubMed: 14991002]
5. Nourry C, Grant SG, Borg JP. Sci STKE 2003;2003(179):RE7. [PubMed: 12709532]
6. Ehlers MD. Nat Neurosci 2003;6(3):231–242. [PubMed: 12577062]
7. Yi JJ, Ehlers MD. Neuron 2005;47(5):629–632. [PubMed: 16129392]
8. DiAntonio A, Hicke L. Annu Rev Neurosci 2004;27:223–246. [PubMed: 15217332]
9. Hariharan IK, Bilder D. Annu Rev Genet 2006;40:335–361. [PubMed: 16872256]
10. Terai T, Nishimura N, Kanda I, Yasui N, Sasaki T. Mol Biol Cell 2006;17(5):2465–2475. [PubMed: 16525024]
11. Lu H, Bilder D. Nat Cell Biol 2005;7(12):1232–1239. [PubMed: 16258546]
12. Giallourakis C, Cao Z, Green T, Wachtel H, Xie X, Lopez-Illasaca M, Daly M, Rioux J, Xavier R. Genome Res 2006;16(8):1056–1072. [PubMed: 16825666]
13. Su AI, Wiltshire T, Batalov S, Lapp H, Ching KA, Block D, Zhang J, Soden R, Hayakawa M, Kreiman G, Cooke MP, Walker JR, Hogenesch JB. Proc Natl Acad Sci U S A 2004;101(16):6062–6067. [PubMed: 15075390]
14. Bartee E, Mansouri M, Hovey Nerenberg BT, Gouveia K, Fruh K. J Virol 2004;78(3):1109–1120. [PubMed: 14722266]
15. Rhodes DR, Yu J, Shanker K, Deshpande N, Varambally R, Ghosh D, Barrette T, Pandey A, Chinnaiyan AM. Neoplasia 2004;6(1):1–6. [PubMed: 15068665]
16. Nakamura N, Fukuda H, Kato A, Hirose S. Mol Biol Cell 2005;16(4):1696–1710. [PubMed: 15689499]
17. Lehner PJ, Hoer S, Dodd R, Duncan LM. Immunol Rev 2005;207:112–125. [PubMed: 16181331]
18. Wu H, Reuver SM, Kuhlendahl S, Chung WJ, Garner CC. J Cell Sci 1998;111(Pt 16):2365–2376. [PubMed: 9683631]
19. Xavier R, Rabizadeh S, Ishiguro K, Andre N, Ortiz JB, Wachtel H, Morris DG, Lopez-Ilasaca M, Shaw AC, Swat W, Seed B. J Cell Biol 2004;166(2):173–178. [PubMed: 15263016]
20. Lue RA, Marfatia SM, Branton D, Chishti AH. Proc Natl Acad Sci U S A 1994;91(21):9818–9822. [PubMed: 7937897]
21. Muller BM, Kistner U, Veh RW, Cases-Langhoff C, Becker B, Gundelfinger ED, Garner CC. J Neurosci 1995;15(3 Pt 2):2354–2366. [PubMed: 7891172]
22. Mantovani F, Banks L. J Biol Chem 2003;278(43):42477–42486. [PubMed: 12902344]
23. Matsumoto Y, Nakagawa S, Yano T, Takizawa S, Nagasaka K, Nakagawa K, Minaguchi T, Wada O, Ooishi H, Matsumoto K, Yasugi T, Kanda T, Huibregtse JM, Taketani Y. J Med Virol 2006;78(4):501–507. [PubMed: 16482544]
24. Ardley HC, Robinson PA. Essays Biochem 2005;41:15–30. [PubMed: 16250895]
25. Fukata M, Fukata Y, Adesnik H, Nicoll RA, Bredt DS. Neuron 2004;44(6):987–996. [PubMed: 15603741]
26. Huang K, Yanai A, Kang R, Arstikaitis P, Singaraja RR, Metzler M, Mullard A, Haigh B, Gauthier-Campbell C, Gutekunst CA, Hayden MR, El-Husseini A. Neuron 2004;44(6):977–986. [PubMed: 15603740]
27. Fallon L, Moreau F, Croft BG, Labib N, Gu WJ, Fon EA. J Biol Chem 2002;277(1):486–491. [PubMed: 11679592]
28. Hoer S, Smith L, Lehner PJ. FEBS Lett 2007;581(1):45–51. [PubMed: 17174307]
29. Singh RK, Iyappan S, Scheffner M. J Biol Chem 2007;282(15):10901–10907. [PubMed: 17301054]
30. Matsuki Y, Ohmura-Hoshino M, Goto E, Aoki M, Mito-Yoshida M, Uematsu M, Hasegawa T, Koseki H, Ohara O, Nakayama M, Toyooka K, Matsuoka K, Hotta H, Yamamoto A, Ishido S. Embo J 2007;26(3):846–854. [PubMed: 17255932]

31. Ohmura-Hoshino M, Goto E, Matsuki Y, Aoki M, Mito M, Uematsu M, Hotta H, Ishido S. J Biochem (Tokyo) 2006;140(2):147–154. [PubMed: 16954532]

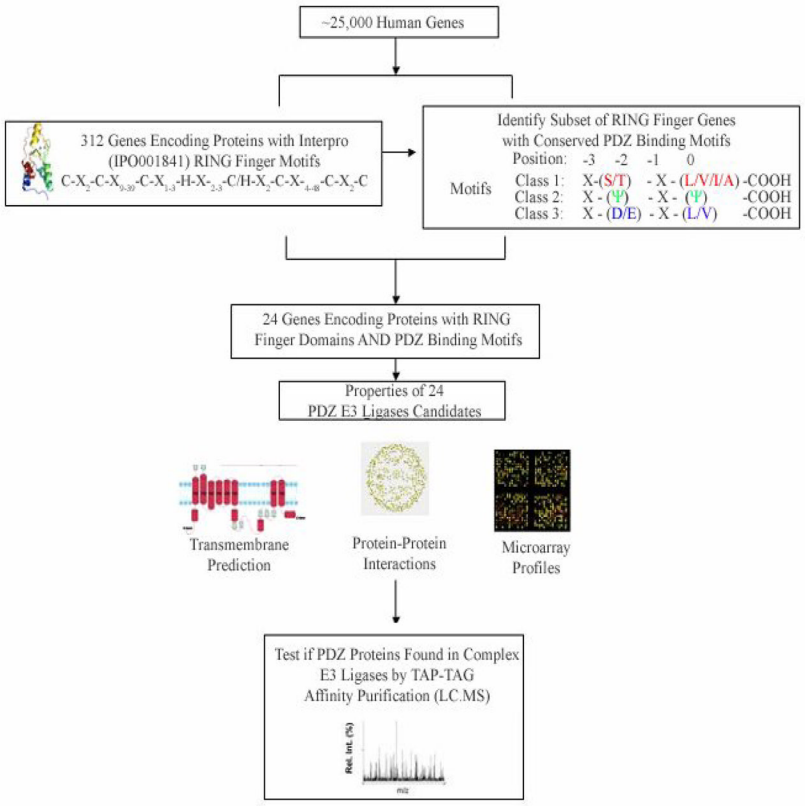

Fig. 1.

Schema for Integrative Genomic Identification of PDZ-E3 Ligase Complexes. The human genome is predicted to harbor approximately 25,000 protein encoding genes. (A) In a subset of proteins, the zinc finger RING (Really Interesting New Gene) domain is known to act as E3 ligases. We analyzed the Interpro database to identify a non-redundant set of 312 genes, which encode for E3 ligase RING domain, including both zinc finger variants C3HC4-type and a C3H2C3-type in the human genome (Supplemental Table I) (B) PDZ domains bind to one of three known classes of consensus carboxy terminal motifs as shown (X representing any amino acid, ψ representing hydrophobic amino acid). We then identified the subset of genes, which encode a RING domain and also contain an evolutionary conserved consensus PDZ binding motif across four mammalian species (human, dog, rat, mouse). (C) This analysis revealed that 24 genes encode RING domains AND harbor PDZ evolutionary conserved PDZ binding motifs restricting or target set of PDZ binding E3 ligases to approximately 0.1% (24/25,000) of the genome. (D) In order to gain insights the cellular location, tissue expression pattern, and pathways in which this compendium of E3 ligases, and more specifically the 24 member subset we analyzed a number of their molecular properties including 1) the potential for transmembrane topology using THMM (Supplemental Table 1), protein-protein interactions based on the BIND database, 3) their expression profiles across 79 human normal human tissue/cell tissues (Supplemental Figure 2) and 4) the phylogenetic relationship among the our 24 target subset using protein alignment (Supplemental Figure 1). Among several properties we identified that 24% (6/24) belong to the transmembrane family of MARCH E3 ligases. (E) To evaluate if our computational algorithm identified bona fide E3 ligases capable of interacting with PDZ domain encoding proteins in an unbiased fashion, we purified protein complexes binding to MARCH2 E3 ligases using tandem affinity purification experimentally verifying the our strategy as described.

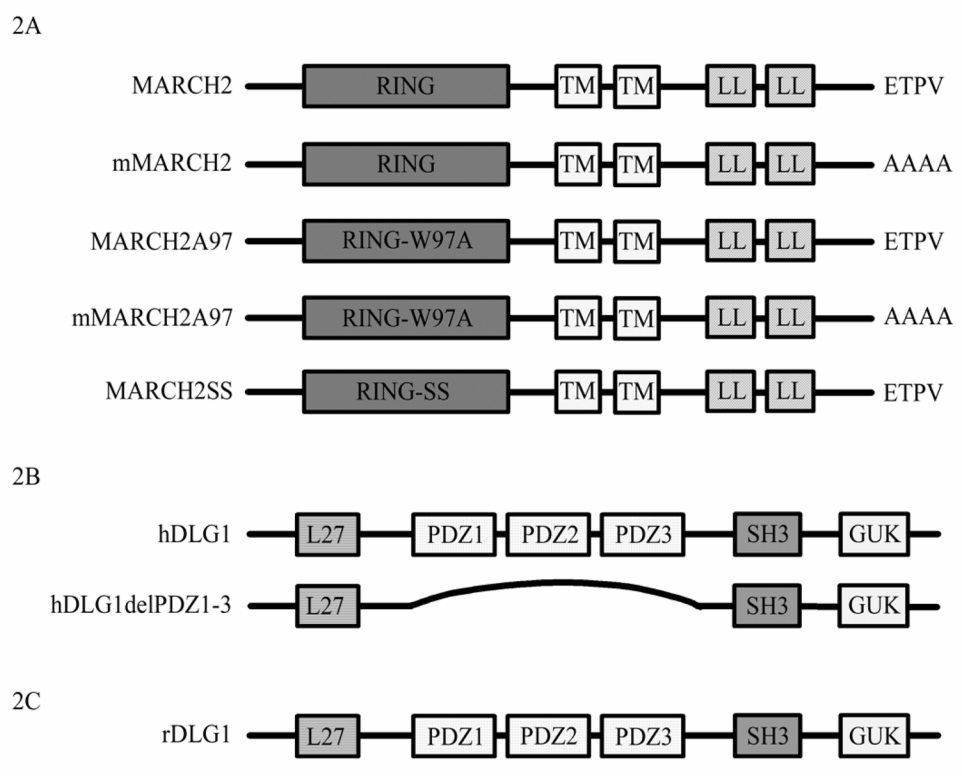

Fig. 2.

Schematic diagram of MARCH2 and DLG1 Constructs. 2A. Schematic representation of MARCH2. TM: transmembrane domain; LL: dileucine motif; ETPV: last four C-terminal residues of MARCH2, a PDZ binding motif (indicated by a line); RING-W97A: the W97 residue in RING domain was replaced with A; RING-SS: conserved C64, C67, C106 and C109 residues in RING domain were replace with S, respectively. 2B. Schematic representation of human DLG1. hDLG1delPDZ1–3: deleted PDZ domains 1–3. 2C: Schematic representation of rat DLG1.

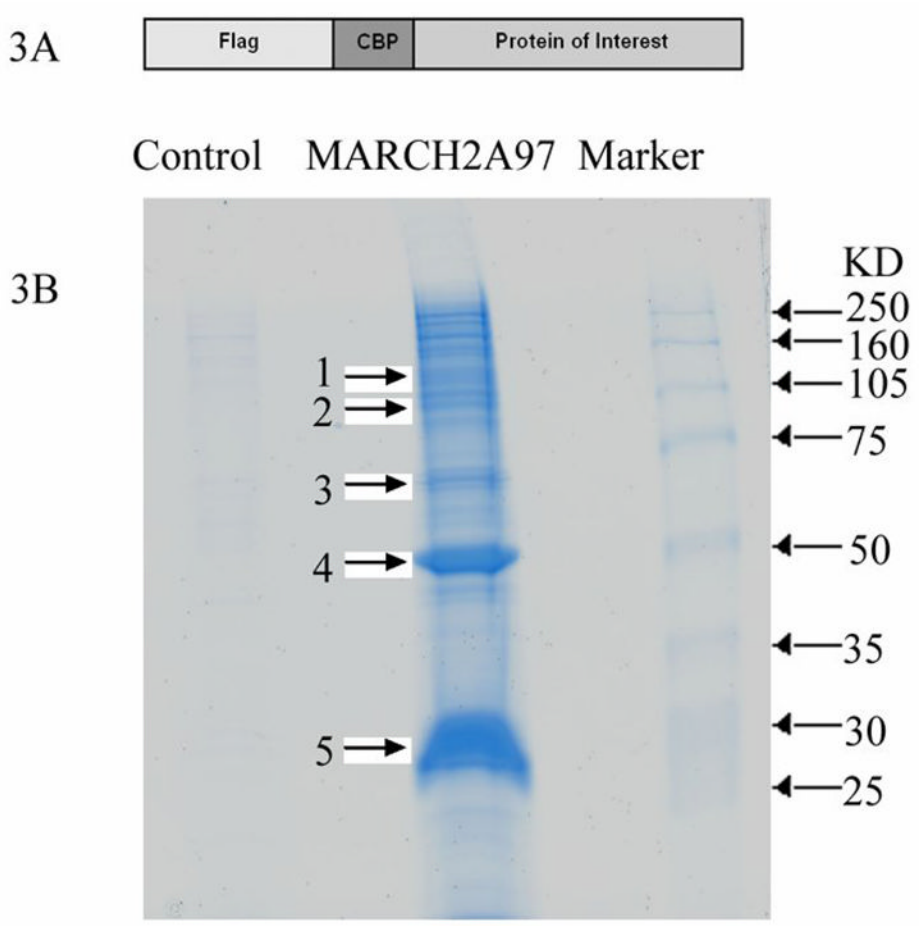

Fig. 3.

Identification of MARCH2 Associated Proteins by TAP Purification. 3A. Schematic representation of a protein of interest with an amino-terminal TAP tag that is composed of the Flag epitope and a calmodulin binding peptide. 3B. Coomassie-stained protein bands co-purified with Flag-CBP-MARCH2A97. Control: purification from original tetracycline-inducible HEK293 cell line; MARCH2A97: purification from Flag-CBP-MARCH2A97 stable cell line; Marker: protein molecular weight marker. Bands 1–4: identified by mass analysis; Band 5: Flag-CBP-MARCH2 protein itself; Band1: containing two bands; Band 2: containing 3 bands; Band 3: containing 2 bands.

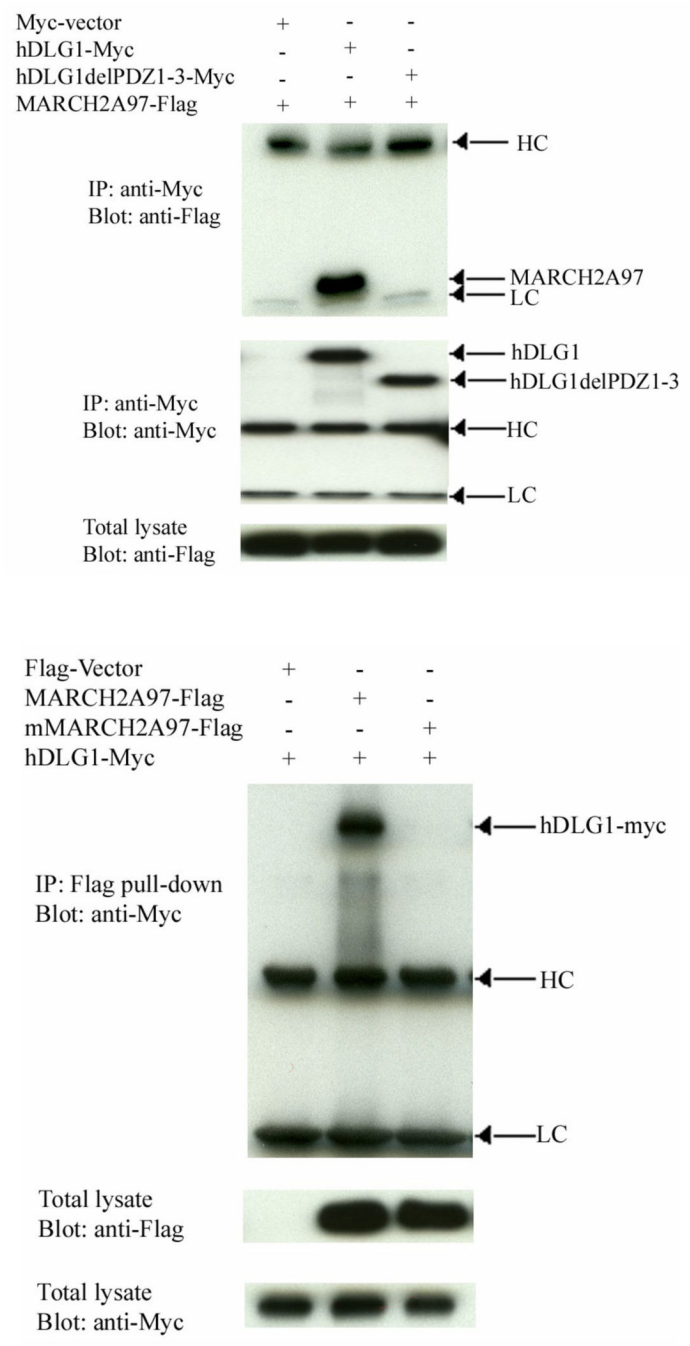

Fig. 4.

MARCH2 interacts with hDLG1. MARCH2A97 (or mMARCH2A97) and hDLG1 (or hDLG1delPDZ1–3) were expressed in HEK293T cells either together or individually (as indicated). 24 h after transfection, the expressed proteins were immunoprecipitated with an anti-Myc antibody (4A) or Flag pull down (4B), and probed with the indicated antibodies.

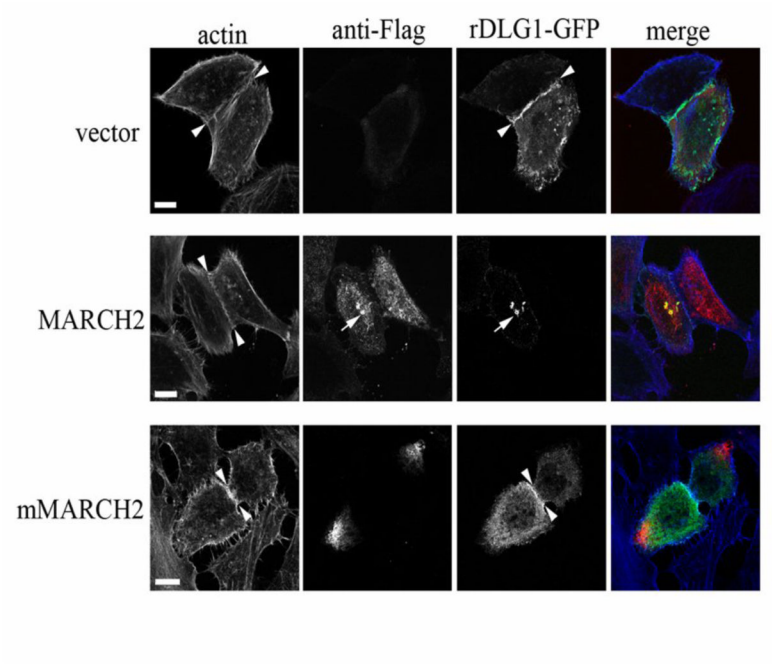

5A

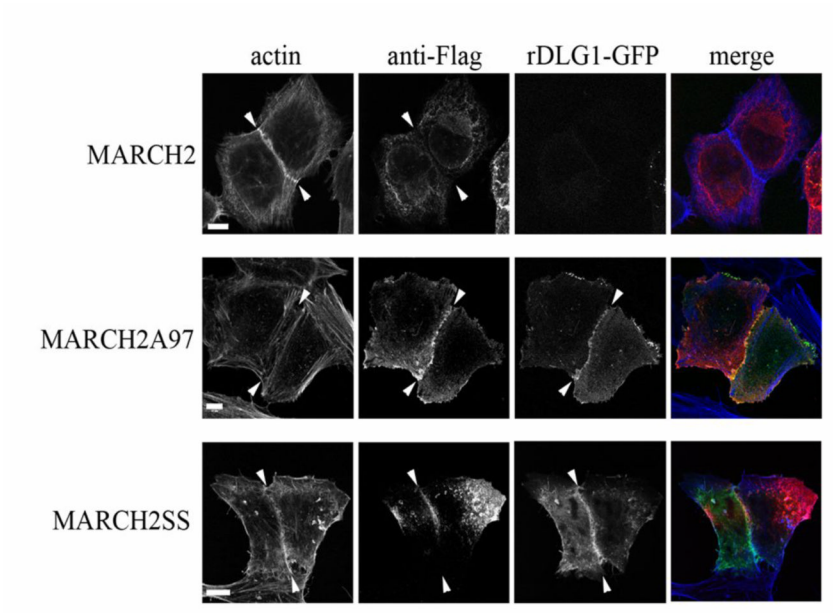

5B

Fig. 5.

MARCH2 Mutants Reveal Differential Roles for PDZ Binding and E3 Ligase Activities. 5A. Expression of wild-type MARCH2-Flag, but not mMARCH2-Flag results in loss of rDLG1-GFP from cells and cell-cell contacts. HeLa cells expressing an rDLG1-GFP fusion and either: empty Flag vector; wild-type MARCH2-Flag or mMARCH2-Flag are shown (in merged images rDLG1-GFP is green, anti-Flag red and actin blue). Actin-rich cell-cell contacts are visible in all three panels (between arrowheads) and co-locate with rDLG1-GFP in vector and mMARCH2 transfected cells. However, rDLG1-GFP is lost from cell-cell contacts when co-transfected with wild-type MARCH2. Co-transfected MARCH2-Flag and rDLG1-GFP co-locate in a perinuclear location (arrowed). In contrast, co-expression of mMARCH2-Flag and

rDLG1-GFP, maintained rDLG1 concentrations at cell contacts with mMARCH2-Flag often polarized in opposition to cell-cell contacts.

5B. E3 ligase negative MARCH2 mutants fail to deplete rDLG1-GFP, but co-locate with rDLG1-GFP at cell-cell contacts. HeLa cells expressing an rDlg1-GFP fusion and either: wild-type MARCH2-Flag; MARCH2A97-Flag or MARCH2SS-Flag are shown (in merged images rDLG1-GFP is green, anti-Flag red and actin blue). Wild-type MARCH2-Flag depleted cells of rDLG1-GFP almost completely and did not localize to cell-cell contacts (between arrowheads). In contrast, both MARCH2A97 and SS mutations failed to deplete rDLG1-GFP in cells, despite comparable expression levels to wild-type MARCH2. Both MARCH2A97 and SS could be co-located with rDLG1-GFP at cell-cell contacts (between arrowheads). Images are representative confocal optical sections of transiently transfected HeLa cells at an original magnification of x63. The scale bar represents 10μm.

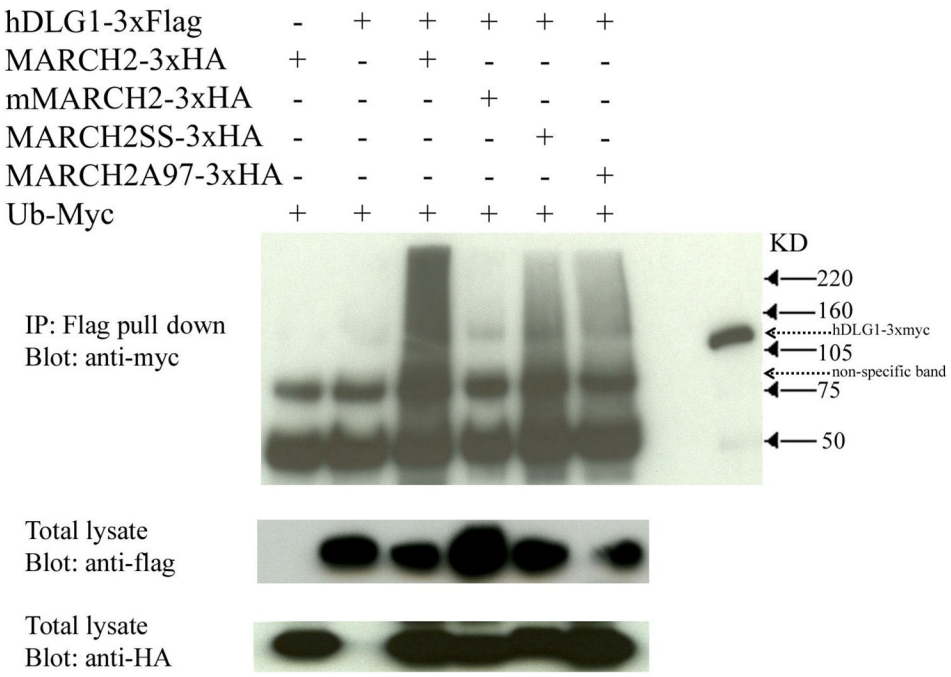

Fig. 6.

MARCH2 Mediates the Ubiquitination of DLG1. H1299 cells in 10-cm plates were co-transfected with indicated plasmids. 24 hours after transfection, cells were harvested and lysed; lysates were incubated with anti-Flag M2-agarose beads and the immunoprecipitated proteins and total cell lysates were applied to SDS gels and blotted for Western blot analysis. The indicated band in the far right lane is total lysate of hDLG1–3xMyc over-expressed in H1299 cell as control to indicate the apparent molecular weight of hDLG1–3xFlag.